Feld, M. S. *Spectrochim. Acta.* **1989**, *45A*, 96.
4. Alfano, R. R.; Tang, G. C.; Pradhan, A.; Lam, W.; Choy, D. S. J.; Opher, E. *IEEE J. Quantum Elec.* **1987**, *23*, 1806.
5. *Arterioisclerosis, Report of the working group on Arteriosclerosis of the National Heart, Lung and blood Institute*; DHHS-NIH Publication No. 81-2034: Washington, U. S. A., 1981; Vol. 1.
6. Braunwald, E., Ed.; *Heart Disease: A textbook of Cardiovascular Disease*; second ed.; W. B. Saunders Co., 1984.
7. *1989 Heart Facts*, American Heart Association, 1988.
8. Letokhov, V. S. *In Laser Picosecond Spectroscopy and Photochemistry of Biomolecules*; Letokhov, V. S., Ed.; Adam Hilger: Bristol, 1987; p 1-55.
9. Chang, M. C.; Petrich, J. W.; Mcdonald, D. B.; Fleming, G. R. *J. Am. Chem. Soc.* **1983**, *105*, 3819.
10. Hochstrasser, R. M.; Negus, D. K. *Proc. Natl. Acad. Sci. U. S. A.*, **1984**, *81*, 4339.
11. D. V. O'Connor and D. Phillips, Time-Correlated Single Photon Counting, Academic Press, Orlando, FL, U. S. A., 1984.
12. Fujimoto, D.; Akiba, K.-Y.; Nakamura, N. *Biochem. Biophys. Res. Commun.* **1977**, *76*, 1124.
13. Gallop, P. M., Blumenfeld, O.: Deifter, S. *Ann. Rev. Biochem.* **1972**, *41*, 618.

Studies of Nonstoichiometry and Physical Properties of the Perovskite $Sr_xHo_{1-x}FeO_{3-y}$ System

Kwang Sun Ryu, Sung Joo Lee, and Chul Hyun Yo

Department of Chemistry, Yonsei University, Seoul 120-749
Received November 8, 1993

Perovskite type oxides of the $Sr_xHo_{1-x}FeO_{3-y}$ system with compositions of $x=0.00$, 0.25, 0.50, 0.75, and 1.00 have been prepared at 1200℃ in air. X-ray powder diffraction assigns the compositions with $x=0.00$ and 0.25 to the orthorhombic crystal system and those with $x=0.50$, 0.75, and 1.00 to the cubic one. The unit cell volumes of solid solutions increase with x in the system. Nonstoichiometric chemical formulas were determined by Mohr salt titration. The mole ratio of Fe^{4+} ions to total iron ions and the concentration of oxygen ion vacancies increase with x. Mössbauer spectra for the compositions of $x=0.00$, 0.25, and 0.50 show six lines indicating the presence of Fe^{3+} ions in the octahedral site. However, the presence of Fe^{4+} ions may also be detected in the spectra for the compositions with $x=0.25$ and $x=0.50$. In the compositions with $x=0.75$ and 1.00, single line patterns show also the mixed valence state of Fe^{3+} and Fe^{4+} ions. The electrical conductivity in the temperature range of −100℃ to 100℃ under atmospheric air pressure increases sharply with x but the activation energy decreases with the mole ratio of Fe^{4+} ion. The conduction mechanism of the perovskite system seems to be hopping of the conduction electrons between the mixed valence iron ions.

Introduction

The atomic arrangement in the perovskite ABO_3 structure was first found for the mineral perovskite, $CaTiO_3$[1]. The unit cell of $CaTiO_3$ could be represented by calcium ions at the corners of a cube with titanium ions at the body center and oxygen ions at the center of the faces. In the perovskite structure, the A cation is coordinated with twelve oxygen ions and the B cation with six oxygen ions. Thus, the A cation is normally found to be somewhat larger than the B cation. In order to have contact between the A, B, and O ions, R_A+R_O should equal to $\sqrt{2}(R_B+R_O)$, where R_A, R_B, and R_O are the ionic radii.

The orthoferrites with the formulae $RFeO_3$, where R is a rare earth metal, have the space group $P_{bnm}(D_{2h})$. Their structure may be viewed as a distorted perovskite structure with four equivalent iron ions per unit cell. The Mössbauer spectra of various orthoferrites have been studied between room temperataure and the Néel temperature(T_N) by Eibschutz *et al.*[2], giving six-line spectra below T_N and single-line spectra above T_N. The Mössbauer spectra of the $SrFeO_x$[3]($x=$ 2.50, 2.60, 2.86, and 3.00) have been analyzed at 4°K, 78°K, and 300°K. Yamamura and Kiriyama[4] have studied the Mössbauer spectra and X-ray diffraction patterns of the $Sr_{1-x}La_xFeO_{2.5+x/2}$ system. Their results showed the existence of a five coordinated iron site surrounded by a trigonal bipyramid of oxygen at $0.2\leq x\leq 0.7$.

$LaFeO_3$ shows the orthorhombic crystal system with four $LaFeO_3$ perovskite units[5] and its neutron-diffraction spectra indicate that it has a G-type[6], spin-ordered antiferromagnetic structure below its Néel temperature of 750 K.

Mössbauer spectra of the $Sr_xDy_{1-x}FeO_{3-y}$ ferrite system have also been analyzed[7]. The Néel temperature of antiferromagnetic $LaFeO_3$ decreases with increasing Sr^{2+} ion concentration. Nonstoichiometric perovskite-related ferrites of composition $La_{1-x}Sr_xFe^{3+}_{1-\tau}Fe^{4+}{}_\tau O_{3-y}$($0\leq x\leq 0.95$) have been studied by Wattiaux *et al*[8]. Due to the mixed valence state of Fe^{3+} and Fe^{4+} ions[9], the electrical conductivity of the perovskite annealed in oxygen is higher than that annealed *in vacuo*. Electrical conductivity of $LaFeO_3$ and $La_{1-x}Sr_xFeO_3$ ($x=0$. 1, 0.25) was studied by Mizusaki *et al*[10-11]. They found that the electronic conduction appeared to be *n*-type in the lower

Table 1. Lattice parameters, reduced unit cell volume, and crystal phase of the $Sr_xHo_{1-x}FeO_{3-y}$ system

Lattice Parameter (Å)				*V*(reduced)	Phase
x	*a*	*b*	*c*		
0.00	5.275 (± 3.295)*	5.581 (± 3.002)	7.585 (± 5.229)	55.82	orthorhombic
0.25	5.285 (± 4.488)	5.587 (± 3.933)	7.603 (± 7.654)	56.12	orthorhombic
0.50	3.856 (± 1.535)	–	–	57.33	cubic
0.75	3.867 (± 0.305)	–	–	57.83	cubic
1.00	3.872 (± 1.201)	–	–	58.07	cubic

*standard deviation unit = 10^{-4}

$P(O_2)$ range and *p*-type in a higher $P(O_2)$ range, and occured by a hopping-type conduction mechanism.

The $Sr_xLa_{1-x}FeO_{3-y}$ system and a number of typical perovskites in which the A site of the ABO_3 is occupied by Sr, Ca, Ba, and La have been studied. However, no systematic study on $HoFeO_3$ has been carried out so far. In the present study, solid solutions of the $Sr_xHo_{1-x}FeO_{3-y}$ system (x=0.00, 0.25, 0.50, 0.75, and 1.00) have been prepared. The cell parameters and the crystal system were determined by X-ray powder diffraction method and the mixed valence state was analyzed and identified by Mohr salt titration and Mössbauer spectroscopy, respectively. The electrical conductivity of the system was also studied as it relates to the x value, the mixed valence state, and the oxygen nonstoichiometry.

Experimental

The starting materials such as Ho_2O_3(99.99%), Fe_2O_3(99.99 %), and $SrCO_3$(99.9%) were weighed in the desired proportions and thoroughly mixed in an agate mortar. The mixture was heated at 1200℃ for 48 hrs and then quenched in the air. The weighing, grinding, and heating processes were repeated three times in order to obtain homogeneous solid solutions. Each powder product was pressed into a pellet under a pressure of 2 ton/cm^2 for 5 min.

X-ray diffraction was carried out using monochromated Cu K α (λ=1.5418 Å) radiation in a range of $15° \le 2\theta \le 75°$ by scanning at 0.04 degree per second. Fe^{2+} ions in a Mohr salt solution are oxidized to Fe^{3+} ions by electron transfer to the Fe^{4+} ions in the sample. The remaining Fe^{2+} ions in the solution are titrated with 0.1 N $K_2Cr_2O_7$. The concentration of Fe^{4+} ions or the τ value in the formulae $La_{1-x}Sr_x$-$Fe^{3+}_{1-\tau}Fe^{4+}_{\tau}O_{3+y}$, could be obtained by the titration. The concentration of oxygen vacancies, $y=(x-\tau)/2$, is calculated from the x and τ values. Knowing the values of x, τ, and y, the nonstoichiometric chemical formulas are determined.

The Mössbauer spectra were recorded by a spectrometer equipped with a 308-channel pulse-height analyzer. The radiation source was Co^{57}(Rh) with 14.4 KeV γ-radiation. Absorbers with a diameter of 25.4 mm and a thickness of 0.5 mm were prepared from the highly ground oxide samples and α-Fe was used as the velocity reference. The Mössbauer spectra of all samples were measured at room temperature.

The electrical conductivity was measured by the D. C. four probe[12] method in a temperature range of −100 to 100℃ under an atmospheric pressure of He gas. The inner two probes, connected to the potentiometer, and the outer two, connected to the electrometer, were used to measure the voltage and the current, respectively. The temperature was raised at the rate of 1℃/min for maintaining thermal equilibrium. The electrical conductivity was calculated by Laplume' s equation[12] and the activation energy was estimated from the slope of the Arhenius plot of the conductivity.

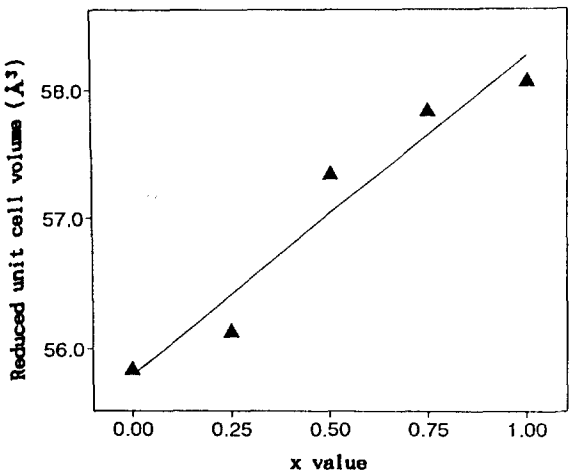

Figure 1. Plot of reduced unit cell volume *vs.* x value for the $Sr_xHo_{1-x}FeO_{3-y}$ system.

Results and Discussion

The X-ray diffraction results indicate that the structure of the compositions with x=0.00 and 0.25 belongs to the orthorhombic crystal system, corresponding to a distorted perovskite structure, and those with x=0.50, 0.75, and 1.00 show the undistorted cubic structure as listed in Table 1. In general, when an alkaline earth metal ion is substituted for a rare earth ion in this structure, either an Fe^{3+} ion must be oxidized to Fe^{4+} or half an oxygen vacancy must be formed in order to satisfy the electroneutrality condition. Table 2 indicates that Fe^{4+} ions and oxygen vacancies occur in nearly equal concentrations to maintain electroneutrality with the substitution of Sr^{2+} ions for Ho^{3+} ions over the entire range of concentrations $0.25 \le x \le 1.00$. The reduced lattice volume increases with x in accordance with Vegard's law as shown in Figure 1.

The unit cell volume of a sample is affected by the metal ions, ligands and their sizes, ionic radii, and vacancy concentrations[13-15]. Among these, the major factors are classified

Table 2. The τ value, y value, nonstoichiometric chemical formulae, and activation energy for the $Sr_xHo_{1-x}FeO_{3-y}$ system

x	τ*	y	Nonstoichiometric chemical formulae	activation energy (eV)
0.00	0.00	0.00	$HeFeO_{3.00}$	0.76
0.25	0.09	0.08	$Sr_{0.25}Ho_{0.75}Fe^{3+}_{0.91}Fe^{4+}_{0.09}O_{2.92}$	0.40
0.50	0.14	0.18	$Sr_{0.50}Ho_{0.50}Fe^{3+}_{0.86}Fe^{4+}_{0.14}O_{2.82}$	0.34
0.75	0.23	0.26	$Sr_{0.75}Ho_{0.25}Fe^{3+}_{0.77}Fe^{4+}_{0.23}O_{2.74}$	0.27
1.00	0.32	0.34	$SrFe^{3+}_{0.68}Fe^{4+}_{0.32}O_{2.66}$	0.10

*Maximum deviation of τ value = ± 0.002

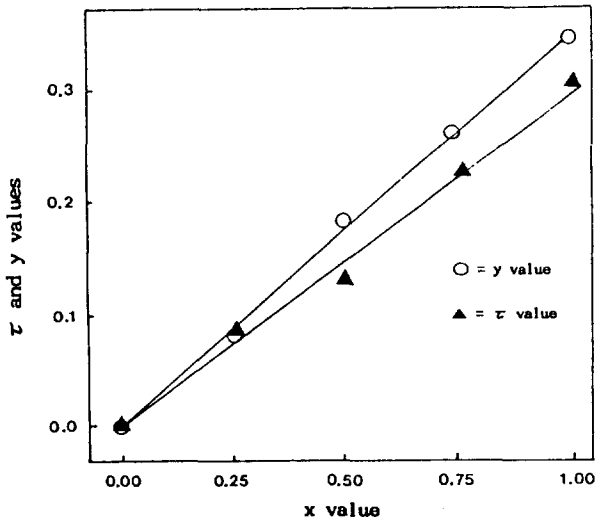

Figure 2. Plots of τ and y values vs. x value for the $Sr_xHo_{1-x}FeO_{3-y}$ system.

into two: first, the increase in ionic bond length due to the substitution of Sr^{2+} for Ho^{3+}, thus increasing the unit cell volume; second, the formation of Fe^{4+} and oxygen vacancies to fulfill the electroneutrality condition. When the Fe^{4+}, which has a smaller ionic radius than Fe^{3+}, is formed, the bond length between Fe and O decreases, and thus the unit cell volume decreases. The structure and the physical properties of solid solutions are affected by the temperature and the oxygen partial pressure during sample preparation. For solid solutions sintered at 1200℃ under atmospheric pressure, the first factor is predominant in these samples; the more Sr is substituted, the larger the unit cell volume.

The τ value, y value, and nonstoichiometric chemical formula as a function of x are listed in Table 2. The τ and y values increase linearly with x as shown in Figure. 2. The results show that $HoFeO_3$ ($x=0.00$) is a stoichiometric compound and the other samples corresponding to the compositions of $0.25 \leq x \leq 1.00$ are nonstoichiometric compounds. The concentration of oxygen vacancies, y, depends on x as well as the temperature and oxygen pressure during sample preparation. Thus the $SrFeO_{2.66}$ ($x=1.00$) is formed under these preparation conditions.

At room temperature, Mössbauer spectra for the compositions of $x=0.00$, 0.25, and 0.50 and the compositions of $x=$ 0.75 and 1.00 are shown in Figure 3 and Figure 4, respectively. The spectra for $x=0.00$, 0.25, and 0.50 compositions are split into six lines by the antiferromagnetic interaction between neighboring iron ions at room temperature, and the Fe^{3+} ion is known to be located in the octahedral site[2] from the internal magnetic field value, H_{int}. The spectra for the $x=0.75$ and 1.00 compositions are not split at room temperature, indicating that these compositions are paramagnetic. The spectra for $x=0.25$ is very similar to that of $x=0.00$ but the symmetry of the six lines is less distinguishable. The six lines in the spectra for $x=0.50$ are beginning to merge into a single line, which means that the Néel temperature is only slightly above room temperature. The spectra for the compositions of $x=0.75$ and 1.00 are single line patterns, which means that the Néel temperature is below room

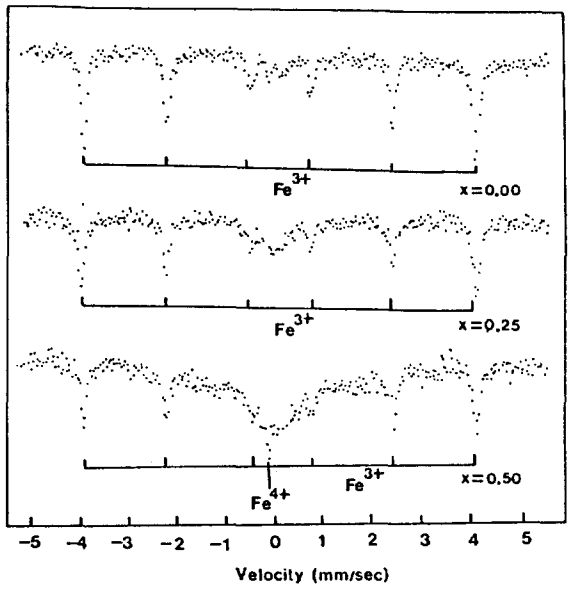

Figure 3. Mössbauer spectra of the compositions of $x=0.00$, 0.25, and 0.50 for the $Sr_xHo_{1-x}FeO_{3-y}$ system.

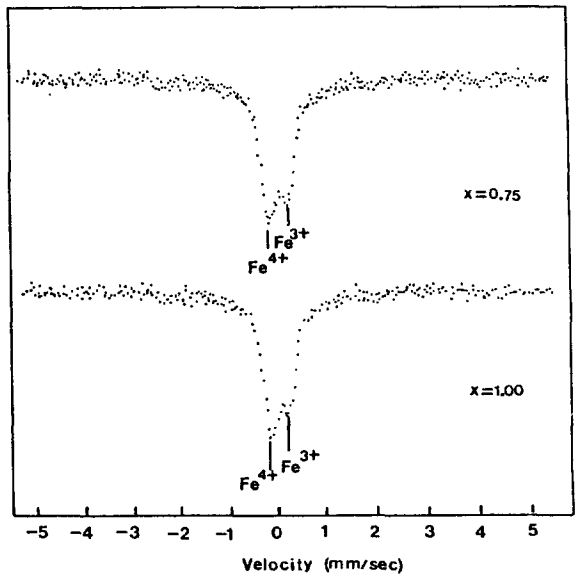

Figure 4. Mössbauer spectra of the compositions of $x=0.75$ and 1.00 for the $Sr_xHo_{1-x}FeO_{3-y}$ system.

Table 3. Mössbauer parameters for compositions of the $Sr_xHo_{1-x}FeO_{3-y}$ system

Composition(x)	Fe type	δ(mm/sec)	ΔEq(mm/sec)	H_{int}(KOe)
0.00	Fe^{3+}	0.237	−0.032	499.8
0.25	Fe^{3+}	0.249	−0.017	499.6
0.50	Fe^{3+}	0.266	0.014	498.2
	Fe^{4+}	−0.214	−	−
0.75	Fe^{3+}	0.437	−	−
	Fe^{4+}	−0.216	−	−
1.00	Fe^{3+}	0.431	−	−
	Fe^{4+}	−0.219	−	−

δ: isomer shift, ΔEq: quadrupole splitting, H_{int}: internal magnetic field

temperature.

Mössbauer parameters for all the compositions of the $Sr_xHo_{1-x}FeO_{3-y}$ system are listed in Table 3. The isomer shift, I.S., of the Fe^{3+} ion increases with the x value up to the composition of $x=0.75$ and then decreases until $x=1.00$. The sudden increase between the compositions of $x=0.50$ and 0.75 is ascribed to the magnetic transition form the antiferromagnetic to the paramagnetic state, agreeing with the result of Shimony *et al*[16]. The I.S. of the Fe^{4+} ion reflects the *s* orbital electron density at the nucleus of the system. Menil[17] suggested that the I.S. should decrease with increasing oxidation number of the iron ion, decreasing coordination number, and increasing electronegativity of the ligand. Since the Fe^{4+} ion is smaller in size and larger in positive electronic charge than the Fe^{3+} ion, the Fe^{4+} ion causes polarization of the electron in the oxygen ion. This polarization increases the covalency in the bond between the Fe^{4+} ion and the oxygen ion. As the covalent character increases and the shielding of the *s* electron by the 3d electrons in the nucleus decreases, the *s* electron density at the nucleus increases and thus the I.S. goes down.

For $x=0.00$, 0.25, 0.50, quadrupole splitting occurs since the electric field acting on Fe nucleus is not constant due to distortion along the *b* axis in the octahedrally coordinated site. The magnitude of the hyperfine internal magnetic field is closely related to the concentration of Fe^{4+} but shows no relation to the nonstoichiometry of oxygen. The magnetic interaction of Fe^{3+}-O-Fe^{3+} is antiferromagnetic. But when Fe^{3+} is oxidized to Fe^{4+}, the number of unpaired electrons decreases and the antiferromagnetic structure is destroyed because of the ferromagnetic Fe^{3+}-O-Fe^{4+} interaction. Therefore, as the concentration of Fe^{4+} increases, the hyperfine internal magnetic field decreases.

The investigation of the temperature dependence of the electrical conductivity provided insight into the physical properties of the perovskite system. The electrical conductivity of the $Sr_xHo_{1-x}FeO_{3-y}$ system increases with increasing temperature as shown in Figure 5. The activation energies calculated from the slopes of plots of log conductivity *vs.* 1000/T are listed in Table 2, and the activation energy is dependent on τ values as shown in Figure 6. The composition of $x=0.00$, which has a zero τ value, has a conductivity between semiconductor and insulator. If the Sr^{2+} ion is substituted for the Ho^{3+} ion in the orthoferrite with low electrical conductivity, some Fe^{3+} ions are oxidized to Fe^{4+} ions and oxygen vacancies are formed to preserve electroneutrality. The electrical conductivity of the compositions with $x>0.00$ would increase due to the hopping of conduction electrons between Fe^{3+} and Fe^{4+} ions.

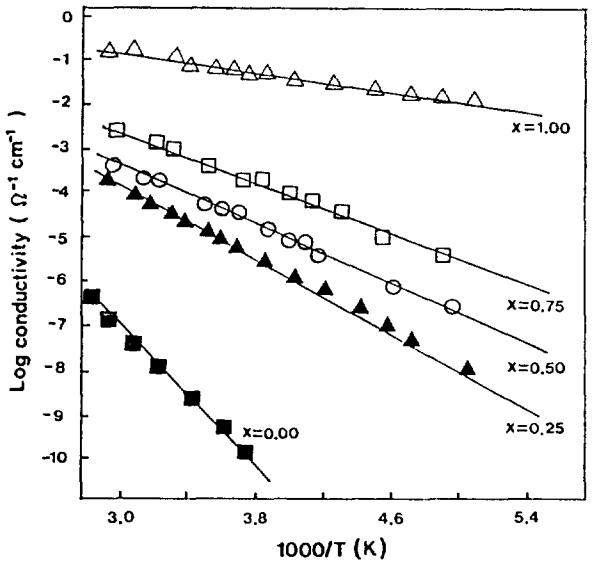

Figure 5. Plots of log conductivity *vs.* 1000/T for the $Sr_xHo_{1-x}FeO_{3-y}$ system.

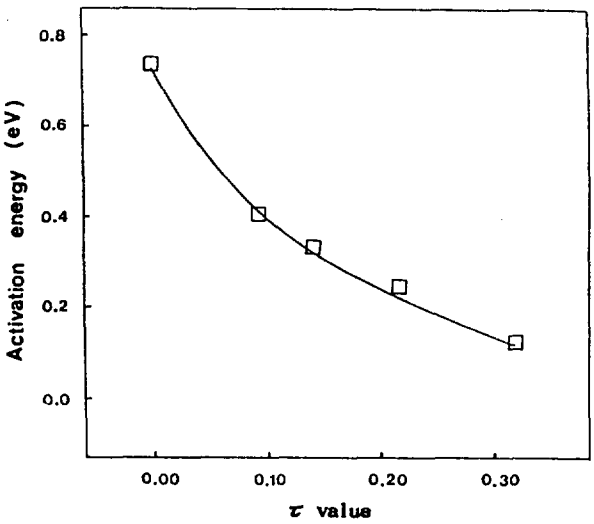

Figure 6. Plot of activation energy *vs.* τ value for the $Sr_xHo_{1-x}FeO_{3-y}$ system.

Generally, since $RFeO_3$ is pictured as the localized model suggested by Goodenough[18], the valence electrons do not form a band and the electrical conductivity is small. But as Fe^{4+} ions begin to form in the solid solution, the electrical conductivity rapidly increases. This is explained by the collective model. It shows that the Fe^{4+} ion is the main factor causing the electrical conductivity of the compound. The electrical conductivity in orthoferrites with mixed cation valences has been studied by many researchers[19,20], and all have come to the conclusion that the high electrical conductivity is due to the hopping of electrons from Fe^{3+} to Fe^{4+}. As

the concentration of Fe^{4+} ions or the Fe^{4+}/Fe^{3+} ratio increases, electrical conductivity is increased in the solid solutions studied in this work. Therefore, the hopping of conduction electrons can be suggested as the electrical conduction mechanism in solid solutions of the system.

Acknowledgments. This works was supported by Grant No. 92-25-00-02 from the Korea Science and Engineering Foundation in 1992 and therefore we express our appreciation to the authorities concerned.

References

1. Galasso, F. S. *Structure, Properties, and Preparation of Perovskite-Type Compounds*; Pergamon Press Ltd.; Oxford, 1968; p 1-11.
2. Eibschutz, M.; Shtrikman, S.; Treves, D. *Mössbauer Studies of Fe^{57} in Orthoferrites; Phys. Rev.* **1967**, *156*(2), 562.
3. Gallagher, P. K.; MacChesney, J. B.; Buchanan, D. N. E. *Mössbauer Effect in the System $SrFeO_{2.5-3.0}$; J. Chem. Phys.* **1964**, *41*, 2429.
4. Yamamura, H.; Kiriyama, R. *Oxygen Vacancies in the Perovskite-type Ferrite. II. Mössbauer Effect in the $SrFeO_{2.5}$-$LaFeO_3$ Solid-Solution System; Bull. Chem. Soc. Japan* **1972**, *45*, 2702.
5. Geller, S.; Wood, E. A. *Crystallographic Studies of Perovskite-like Compounds; I. Rare Earth Orthoferrites and $YFeO_3$, $YCrO_3$, and $YAlO_3$; Acta Cryst.* **1956**, *9*, 563.
6. Wollan, E. O.; Kochler, W. C. *Neutron Diffraction Study of the Magnetic Properties of the Series of Perovskite-Type Compounds $[(1-x)La, xCa]MnO_3$; Phys. Rev.* **1955**, *100*, 545.
7. Yo, C. H.; Lee, E. S.; Pyon, M. S. *Study of the Nonstoichiometry and Physical Properties of the $Sr_xDy_{1-x}FeO_{3-y}$ Ferrite System; J. Solid State Chem.* **1988**, *73*, 411.
8. Wattiaux, A.; Grenier, J. C.; Pouchard, M.; Hagenmuller, P. *Electrolytic Oxygen Evolution in Alkaline Medium on $La_{1-x}Sr_xFeO_{3-y}$ Perovskite-Related Ferrites; J. Electrochem. Soc.* **1987**, *134*(7), 1714.
9. Watanabe, H. *Magnetic Properties of Perovskites Containing Strontium; J. Phys. Soc. Japan* **1957**, *12*, 515.
10. Mizusaki, J.; Sasamoto, T.; Cannon, W. R.; Bowen, H. K. *Electronic Conductivity, Seebeck Coefficient, and Defect Structure of $LaFeO_3$; J. Am. Ceram. Soc.* **1982**, *65*(8), 363.
11. Mizusaki, J.; Sasamoto, T.; Cannon, W. R.; Bowen, H. K. *Electronic Conductivity, Seebeck Coefficient, and Defect Structure of $La_{1-x}Sr_xFeO_3$ ($x=0.1$, 0.25); J. Am. Ceram. Soc.* **1983**, *66*(4), 247.
12. Laplume, J. *Bases Théoriques de la Mesure de la Résistivité et de la Constante de Hall par la Méthode des Pointes; L. onde Elektrique*, **1955**, *335*, 113.
13. Grenier, J. C.; Pouchard, M.; Hagenmuller, P. *Structure and Bonding 47*; Springer-Verlag: Berlin, Heidelberg **1981**.
14. Yakel, H. L. *On the Structures of some Compounds of the Perovskite Type; Acta. Cryst.* **1955**, *8*, 394.
15. Marezio, M.; Remeika, J. P.; Dernier, P. D. *The Crystal Chemistry of the Rare Earth Orthoferrite; Acta. Cryst.* **1970**, *B26*, 2008.
16. Shimony U.; Knudsen, J. M. *Mössbauer Studies on Iron in the Perovskites $La_{1-x}Sr_xFeO_{3-y}(O\leq x\leq 1)$; Phys. Rev.* **1966**, *144*, 361.
17. Menil, F. *Systematic Trends of the ^{57}Fe Mössbauer Isomer Shifts in (FeO_n) and (FeF_n) Polyhedra. Evidence of a new Correlation between the Competing Bond T-X ($\rightarrow Fe$) (Where X is O or F any T and Element with a Formal Positive Charge); J. Phys. Chem. Solids*, **1985**, *46*(7), 763.
18. Goodenough, J. B.; Longo, J. M. *Crystallographic and Magnetic Properties of Perovskite and Perovskite-related Compound*; Landolt-Bornstein: Naue Series III 4a, Springer-Verlag: Berlin, Heidelberg, New York, 1970.
19. Yamamura, H.; Haneda, H.; Shirasaki, S.; Takada, K. *Magnetic and Electrical Properties in the Defect Perovskite System $La_{1-x}Na_xFeO_{3-\delta}$; J. Solid State Chem.* **1981**, *36*, 1.
20. MacChesncy, J. B.; Jetzt, J.; Potter, J. F.; Williams, H.; Sherwood, R. C. *Electrical and Magnetic Properties of the System $SrFeO_3$-$BiFeO_3$; J. Am. Ceram. Soc.* **1966**, *49*, 644.